

## Miniature Integrated Thin Film Solar Cells for Micro Machines

T. Minemoto, Y. Suzuki, T. Kitaura, H. Takakura and Y. Hamakawa

Faculty of Science and Engineering, Ritsumeikan University

1-1-1 Nojihigashi, Kusatsu, Shiga 525-8577, Japan

Tel/Fax: +81-77-561-3938, E-mail minemoto@se.ritsumei.ac.jp

### Abstract

The fabrication flow of miniature integrated solar cells based on amorphous Si (a-Si) is presented. The output estimations of the integrated solar cell under sunlight are calculated. The calculations show that the typical output power of 10  $\mu$ W can be obtained with the output voltage of 10 V and current of 1  $\mu$ A. To overcome the low output power due to the low input power density of sunlight, the application of concentration light has been proposed. The output estimations under concentration light have been done with and without light induced degradation of a-Si solar cells. The results indicate that output powers, thus output voltages and currents, can be controlled with concentration light intensity and the integration number, and the light induced degradation directly affect the output power. We conclude that the development and application of high efficiency thin film solar cells without light induced degradation will be the key to realize miniature integrated thin film solar cells.

*Keywords: solar cell, integration, amorphous Si, thin film, concentration*

### 1 INTRODUCTION

Solar cells are one of the promising power sources for micro-electro mechanical systems (MEMS). Various types of thin film solar cells such as multi-junction amorphous Si (a-Si) solar cells [1], transverse-junction a-Si solar cells [2] and GaAs solar cells [3] were reported for the application in MEMS. Only thin film solar cells have been applied in MEMS because of the capability of making fine monolithic interconnections of solar cells, which required for high voltage, by the sequential thin film deposition and cell separation methods [4]. There are some advantages in the application of solar cells in MEMS. In these advantages, the important features are wire-less power supply, no fuel replenishment and infinite fuel source if sunlight is used. Sunlight gives some advantages but also have a disadvantage which is low energy density compared to other power sources. The possible solution of this problem is the application of high intensity light, e.g., concentration light and laser. In this work, a-Si solar cells were fabricated and measured under sunlight and different light intensities. We present the fabrication flow of the miniature integrated a-Si solar cell, and discuss the output estimations of the solar cells with the area of 0.25 mm<sup>2</sup>,

which is our target in size, under sunlight and concentration light.

### 2 FABRICATION FLOW OF MINIATURE INTEGRATED SOLAR CELL

Figure 1 shows the schematic fabrication flow of miniature integrated a-Si solar cells. First in the step 1, the front electrode of a transparent conductive oxide of SnO<sub>2</sub> and the photovoltaic layer of a-Si with a p-i-n junction are deposited on a glass substrate. In the step 2 and 3, to separate unit cells, a part of the a-Si and SnO<sub>2</sub> layers are removed by the patterning 1 and the patterning 2. In the step 4, the insulator of MgO is deposited to prevent short-circuit between front and back electrodes of the same unit cell. In the step5, the MgO layer is removed by the patterning 3 to expose the a-Si and SnO<sub>2</sub> layers, and in the step 6 the back electrode of Al is deposited. Finally in the step 7, a part of the Al layer is removed to separate unit cells. Incident light irradiates from the glass substrate side and current flows as indicated in the figure. The fabrication of miniature integrated a-Si solar cells by this process is under optimization in our laboratory. In this paper, we focus on the output estimations of the integrated solar cell with this structure.

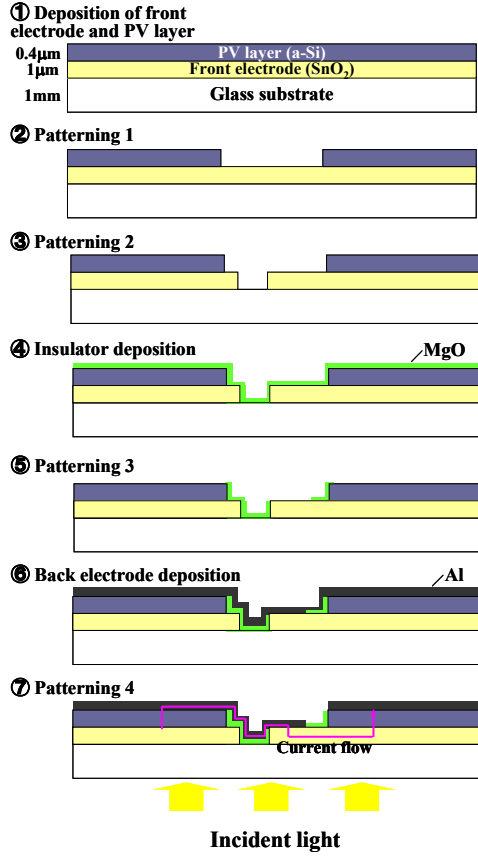


Figure 1. Schematic fabrication flow of miniature integrated a-Si solar cells.

### 3 OUTPUT ESTIMATIONS OF MINIATURE INTEGRATED A-SI SOLAR CELLS

#### 3.1 Unit cell structure and calculation method

Figure 2 shows (a) three-dimensional image and (b) cross-sectional unit cell structure of the miniature integrated a-Si solar cell. Here,  $W_A$  indicates the width of an active area which acts as a solar cell,  $W_D$  dead width which is the sum of the widths of patterning 2  $W_1$  and the patterning 4  $W_2$ , and a SnO<sub>2</sub>/Al contact width  $W_c$ .  $Z$  indicates the length of a unit cell.  $W$  indicates the unit cell width, i.e., the sum of  $W_A$  and  $W_D$ . In this calculation, total cell width and length are assumed to be 0.5 mm, respectively; the total cell area is 0.25 mm<sup>2</sup>. For integration,  $Z$  is fixed and  $W$  is varied with the number of unit cells  $N$ . An output voltage  $V_{out}$  is the product of a unit cell output voltage  $V_{max}$  and  $N$  which determines  $W$  at the same time. An output current  $I_{out}$  is determined by the unit cell area

of the product of  $W_A$  and  $Z$ , current density  $J_{max}$  of a unit cell under an input irradiance  $I_r$ . An output power  $P_{out}$  is the product of  $V_{out}$  and  $I_{out}$ .

$$V_{out} = V_{max} \times N \quad (1)$$

$$I_{out} = W_A \times Z \times J_{max} \quad (2)$$

$$P_{out} = V_{out} \times I_{out} \quad (3)$$

Here,  $V_{max}$  and  $J_{max}$  are obtained by the characteristics of a fabricated a-Si solar cell.  $W_A$  is determined from  $W$ ,  $W_1$ ,  $W_2$  and  $W_c$ .  $W_1$  and  $W_2$  are the width to separate conductive layer to prevent short-circuit so that the values are assumed to be 5 μm, respectively.  $W_c$  determine the contact resistance at a SnO<sub>2</sub>/Al interface.  $R_c$  is given by [5]

$$R_c = (L/Z)R_s \coth(W_c/L) \quad (4)$$

where  $R_s$  is the sheet resistance of the SnO<sub>2</sub> layer and  $L$  is the transfer length of current defined by

$$L = (\rho_c / R_s)^{1/2} \quad (5)$$

where  $\rho_c$  is the contact resistivity of the SnO<sub>2</sub>/Al interface. In this calculation,  $R_s$  and  $\rho_c$  are assumed to be 10 Ω/□ and  $2 \times 10^{-3}$  Ω-cm<sup>2</sup>.  $W_c$  is determined to make the power loss by  $R_c$  of lower than 5%.

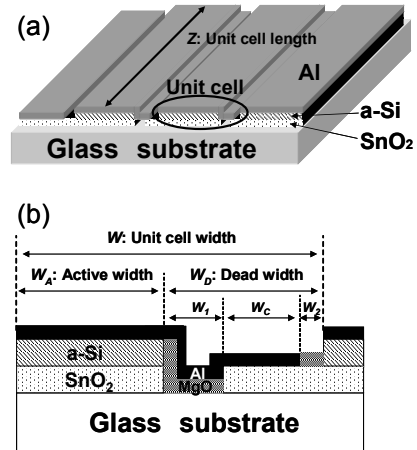


Figure 2 (a) Three-dimensional image and (b) Cross-sectional unit cell structure of the miniature integrated solar cell.

#### 3.2 Output estimation under sunlight

In this section, the output estimations of the miniature integrated a-Si solar cell calculated using the performance of a fabricated a-Si solar cell are discussed. Single a-Si solar cell with the structure of Al/n-a-Si/i-a-Si/p-a-Si/SnO<sub>2</sub>/glass was fabricated. The area of the cell is 0.25 mm<sup>2</sup>. Typical thickness of Al, a-Si and SnO<sub>2</sub> layers are 0.2 μm, 0.4 μm and 1.0 μm, respectively. The measurement of current-voltage

characteristics the a-Si solar cell under the light intensity with  $100\text{mW}/\text{cm}^2$  corresponding to sunlight shows the energy conversion efficiency of 6.65 %,  $J_{max}$  of  $9.30\text{ mA}/\text{cm}^2$  and  $V_{max}$  of 0.715 V. Figure 3 shows the calculated output power and current as a function of output voltage and integration number based on the measurement parameters. The highest output power of  $16.6\text{ }\mu\text{W}$  is obtained at the no-integration. The output power proportionally decreases as the output voltage and integration number increase, because of the increase in the dead area. As can be seen from the figure, the output current shows the highest value of  $23.2\text{ }\mu\text{A}$  for no-integration and that rapidly decreases as the output voltage and integration number increase. This is because all the cells are series connected, and the unit cell area determining the output current rapidly decreases as the integration number increases. For example, if the output voltage of more than 10 V is required, the output current will be lower than  $1\text{ }\mu\text{A}$ . This is the limitation of the a-Si solar cell application in MEMS under sunlight. The use of higher efficiency a-Si solar cells will loosen the limitation; however that is not significant difference.

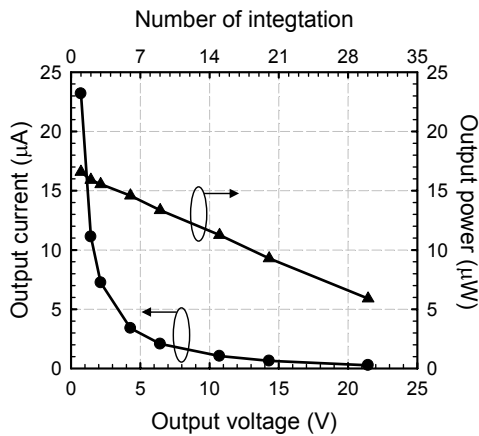


Figure 3 Calculated output power and current as a function of output voltage and integration number under sunlight.

### 3.3 Output estimation under different irradiances

The application of high intensity light, e.g., concentration light and laser, is attractive to increase the outputs. Sunlight has a typical irradiance of  $0.25\text{ mW}$  in  $0.25\text{ mm}^2$ , and that is diffuse light so that the concentration by optical lens will produce higher input powers. There are some reports on high efficiency concentrator solar cells based on GaAs with more than 300 times concentration of sunlight [6]. In this section, the output estimations of the miniature integrated a-Si solar cell under concentration light with different input irradiances are discussed with and without the performance changes of a-Si solar cells with the irradiances.

#### (i) Without performance changes under different irradiances

The estimations of outputs were done under the assumption that the solar cell performance is unchanged with different irradiances, i.e., the cell temperature is controlled by cooling system and there is no light induced degradation in a-Si. Here, the characteristics of the a-Si solar cell described in the section 3.2 are used. Figure 4 shows the calculated output voltage of the solar cell with different irradiances and output currents. For a fixed output current, the curve shapes of the dependence of the output voltages on the input irradiances are similar, and the curve shifts to high irradiances as the output current increases. This indicates both the output voltage and current can be controlled by the input irradiance. As can be seen from the figure, the output voltage is saturated at 35 V which is determined by the dead width of the unit cell of more than  $10\text{ }\mu\text{m}$ . The dead width determines the maximum integration number of 49 for the cell width of  $0.5\text{ mm}$ , and the product of the number and the unit cell output voltage of 0.715 V gives the maximum output voltage of 35 V. This indicates that a maximum output voltage increases as a dead area decreases, e.g., the dead area width is required to be narrower than  $3.5\text{ }\mu\text{m}$  to obtain the output voltage of more than 100 V. From the figure, the attainable output voltage and current under typical concentration lights can be read as summarized in Table 1.

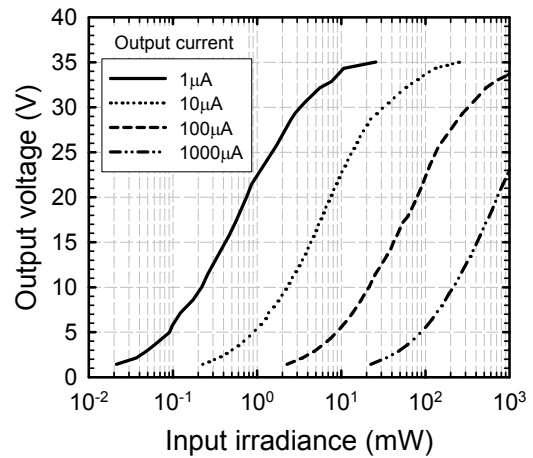


Figure 4 Calculated outputs of the miniature integrated a-Si solar cell with different irradiances.

Table 1. Typical concentrations and estimated outputs.

Concentration	Input irradiance (mW)	Output current ( $\mu\text{A}$ )	Outout voltage (V)
10	2.5	1	28.6
10	2.5	10	10.7
10	2.5	100	1.43
100	25	1	35.0
100	25	10	29.3
100	25	100	10.7
100	25	1000	1.43
300	75	10	32.2
300	75	100	19.3
300	75	1000	4.29

(ii) With performance changes under different irradiances

Figure 5 shows the current-voltage characteristics of the a-Si solar cell with different input irradiances. Fill factors decreases due to the degradation in series and parallel resistances as the input irradiance increases. The decrease in fill factor causes the degradation of  $J_{max}$ /concentration and the energy conversion efficiency. This is the light induced degradation of a-Si solar cells called Staebler-Wronski effect [7]. Figure 6 shows the calculated output current dependence of the input irradiance with and without the light induced degradation. The output current differences, which directly corresponds to the loss of the output power by the degradation, between the calculations with and without the degradation increase with increasing the input irradiance and with decreasing the integration number  $N$ . The output power loss for the

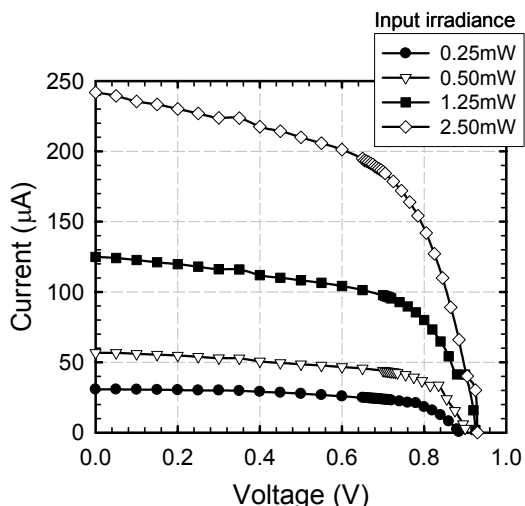


Figure 5. Current-voltage characteristics of the a-Si solar cell under different input irradiances.

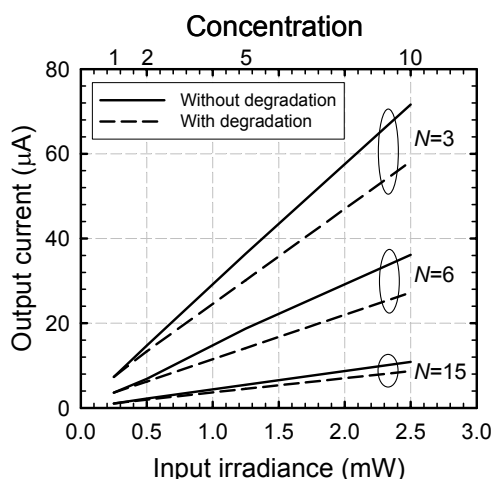


Figure 6. Calculated output current dependence of the input irradiance with and without the light induced degradation.

integration number of 3 under the input irradiance of 2.50 mW is as high as 31.5  $\mu$ W, which is 20.5 % of the total output power without the degradation. If solar cell parameters are unaffected by illumination level, i.e., there is no light induced degradation and the cell temperature is unchanged, a conversion efficiency increases as the illumination concentration increases by the increase of open circuit voltage. Actually, performance improvements are observed in concentrator solar cells based on GaAs [6]. The application of high efficiency thin film solar cells without light induced degradation, such as CuInGaSe<sub>2</sub> [8], will be the key to realize miniature integrated thin film solar cells.

#### 4 SUMMARY

The fabrication flow of miniature integrated solar cells was presented. The output estimation of the a-Si solar cell under the sunlight showed that the typical output power of around 10  $\mu$ W can be obtained. The output estimation without light induced degradation under concentration light showed that the output voltage and current can be controlled by the irradiance, and the typical concentration of 300 times gives as high as 4.29 mW with 4.29 V and 1mA. The estimation with light induced degradation indicated that the decrease in the efficiency directly reduce the output power. The results suggest that the development and application of high efficiency solar cells without light induced degradation will be the key to realize miniature integrated thin film solar cells.

#### ACKNOWLEDGEMENTS

This work was supported by the 21st Century COE program. The authors would like to thank Professors Susumu Sugiyama and Toshiyuki Toriyama for their useful discussion.

#### REFERENCES

- [1] J. B. Lee, et al., Journal of Microelectromechanical systems, 4 (1995) 102.
- [2] M. A. Kroon, et al., Appl. Phys. Lett. 72 (1998) 209.
- [3] J. Ohsawa, et al., Jpn. J. Appl. Phys. 38 (1999) 6947.
- [4] Y. Kuwano, et al., Jpn. J. Appl. Phys. 19 (1980) 137.
- [5] D. K. Schroder, et al., IEEE Transactions on Electron Devices 31 (1984) 637.
- [6] R. R. King, et al., Proc. of the Third World Conference on Photovoltaic Energy Conversion (Osaka, 2003) 622.
- [7] D. L. Staebler and C. R. Wronski, Appl. Phys. Lett. 31 (1977) 292.
- [8] K. Ramanathan, et al., Prog. Photovolt: Res. Appl. 2003; 11:225.